African Multidisciplinary
Journal of Sciences and Artificial Intelligence

ISSN : 0000-0000

Index: Harvard, Boston, Sydney University, Dimensions, Lens, ResearchGet Scilit, Semantic, Google Scholar, Base etc

https://doi.org/10.58578/AMJSAI.v1i1.3370

Synthesis of SiO2/TiO2 Core – Shell Nanofibres for Photodegradation of Hexamethyldisiloxane

E. A. Kamba & E. B Attah Daniel
Federal University Wukari Taraba State. Nigeria
eacambah@gmail.com

Article Info:

Submitted:	Revised:	Accepted:	Published:
Jun 17, 2024	Jul 12, 2024	Jul 14, 2024	Jul 17, 2024

Abstract

As the world faces the increasing energy demands of its growing population a number of novel and renewable energy sources are being investigated as replacement agents for conventional fossil fuel species. In this study SiO2/TiO2 core–shell nanofibres were synthesised and characterised using facile experimental procedures. The synthesized catalyst was utilized for photodecomposition of hexamethyldisiloxane (HMS) in biogas. The results obtained revealed that by the decomposition properties of the created material it was possible to establish a photocatalyst equipped with properties capable of decomposing siloxanes in biogas with high efficiency.

Keywords: Photogradation, Photocatalyst, Siloxanes, Titaniumdioxide, Nanofibres

INTRODUCTION

Even though the many sub-1% contaminants in biogas remain at a very low concentration, a number of them can prove to be very harmful. Of these impurities, two different species of chemicals can be identified as being of particular concern for the usage of biogas as an alternative to conventional fossil fuels; sulfides (and in particular hydrogen sulphide, H_2S) and siloxanes. Hydrogen sulfide is a particularly harmful chemical impurity present in biogas as it remains highly toxic in concentrations as low as parts per billion and upon combustion can convert into highly corrosive species such as sulfur dioxide (SO_2) and sulfuric acid (H_2SO_4) [1]. In the light of this, a number of studies has been undertaken in order to decompose hydrogen sulfide and render biogas a more viable source of combustible fuel [2]. Despite the importance of H_2S as a contaminant in biogas it is also essential to consider the siloxane contaminant species present in biogas as, although only present in minute concentrations, it can prove fatal to mechanical systems utilizing biogas.

One of the major issues with pure titania nanostructures has been recognised as their mechanical weakness to mechanical stress variations. This weakness of titania nanofibres signifies that the durability of a pure titania catalyst would be heavily limited and, furthermore, that catalysts composed of solely titania nanostructures would only supply a very constrained use for industrial applications, both in terms of catalyst lifetime and catalyst mechanical stability. As a consequence of this, the strengthening of titania nanostructures through the introduction of more mechanically resistant materials is a very attractive prospect. Indeed, such structures would allow to maintain the high photocatalytic activity of titania catalysts whilst overcoming the major limitations of nanostructures formed solely of these catalysts.

SiO_2 is an inert material that possesses many advantageous properties, amongst which a relatively high resistance to mechanical and thermal stress. Studies on SiO_2 nanofibres have shown that the construction of SiO_2 nanofibres through electrospinning is a relatively facile, and high yield procedure [3]. These synthetic advantages combined with the mechanical strength displayed by silica nanofibres render SiO_2 an ideal candidate for the creation of gas purification hybrid nanostructures. The creation of SiO_2/TiO_2 hybrid nanofibres was thus chosen for the synthesis of highly catalytic gas purification devices. However, although SiO_2 nanofibres display a number of advantages, SiO_2 is not a photoactive material. As such, the incorporation of SiO_2 nanofibres in a TiO_2 nanofibre

mat would effectively result in a decrease in catalyst photoefficiency. This problem was overcome by the creation of core-shell SiO_2/TiO_2 structures which allowed to maintain the total catalyst exposed surface area in the created materials as a photoactive species whilst remaining mechanically strong.

A number of different procedures have been studied allowing the creation of SiO_2/TiO_2 core-shell structures. Such procedures usually focus on the initial creation of a silica substrate which is then coated by titania through a series of chemical procedures [4]. The coating procedures are usually carried out through the immersion of a substrate into a precursor solution and the subsequent conversion of the precursor into the desired chemical species. These processes are commonly called dip-coating procedures. Dip coating procedures have gained a lot of interest in the formation of complex nanostructures due to their relative simplicity and versatility. A number of complex nanostructures have been synthesised by using these simple dip-coating procedures. The validity of these procedures for the formation of TiO_2 coatings was demonstrated successfully by Nakamura et al, through the dip coating of silica spheres using TiO_2 precursors [4-6]. Further studies also showed validity of dip coating procedures onto electrospun polymer nanofibres [7]. As such, the creation of SiO_2/TiO_2 core – shell nanofibres through dip-coating procedures was chosen as a method to overcome the inherent disadvantages presented by pure titania nanofibres.

METHODS

Synthesis of SiO_2 / TiO_2 Core – Shell Nanofibre

The synthesis for SiO_2/TiO_2 core-shell nanofibres proceeded through two main steps. Firstly SiO_2 nanofibres were created through a standard electrospinning procedure and then the created fibres were dip coated into a titanium precursor solution. The precursor was finally converted into titania allowing for the final synthesis of a TiO_2 shell on the SiO_2 nanofibres.

Phosphoric acid (85% , 50µl) was added dropwise to a solution of TEOS (50 %wt) in deionised water and allowed to stir for 5 hours in order to create an initial SiO_2 gel precursor. The created gel was then added to a solution of PVA (hydrolysed, 11 %wt, MW 85000 – 124000) in deionised water and allowed to stir for a further 2 hours. Finally, the created solution was extruded from a stainless steel syringe needle (23 gauge) through the

means of a high voltage (20 kV) current applied to the needle. A syringe pump was used to inject the created solution into the needle at a constant rate (2 ml/h). The created fibres were collected on a grounded Al rotating drum placed at a fixed distance (25cm) from the needle. Figure 1 shows a schematic representation of the experimental set up used for the nanofibre electrospinning procedure. After the electrospinning procedure was completed, the created fibre mat was then removed from its substrate and placed in a furnace at 900 °C for 14 h in order to remove the PVA framework and create pure SiO_2 nanofibres.

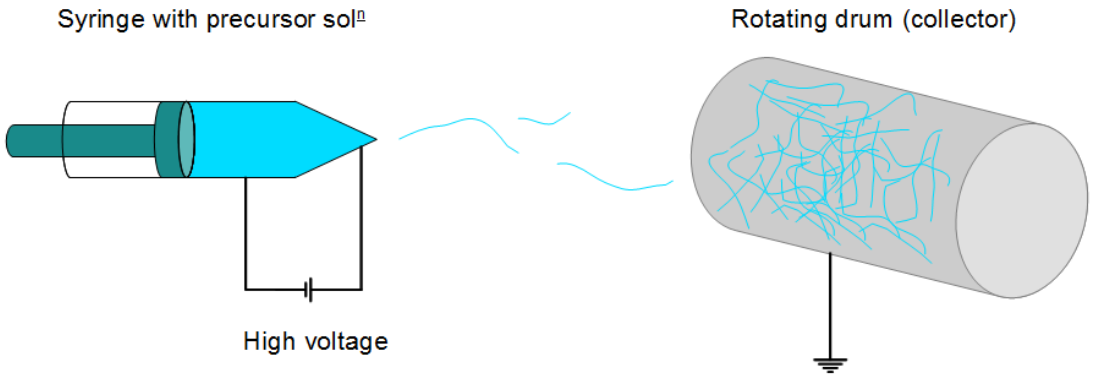

Figure 1: Schematic representation of the experimental set up used for the synthesis of nanofibres

The newly synthesised SiO_2 nanofibres were then covered with TiO_2 layers of controlled thickness by using a simple four step procedure. Firstly, the nanofibres were immersed for 30 minutes into a solution of TT^iP (5 %wt) in IPA, this allowed the adsorption of the titanium precursor onto the surface of the silica. Secondly, in order to clean any non adsorbed excess from the surface of the sample, the fibres were immersed into an IPA solution. Thirdly, the remaining precursor adsorbed on the fibres was hydrolised into $Ti(OH)_2$ by immersing the fibres into deionised water. Finally the excess water in the fibre mat was removed by immersing the sample in IPA. This four step procedure was repeated up to 10 times in order to allow for the formation of multiple shells on the silica nanofibres. Once the dip coating cycle was completed, the samples were allowed to dry in air and placed in a furnace at 550 °C for 3 hours in order to allow for the conversion of the titanium hydroxide into TiO_2 and improve the crystallinity of the sample.

Photodegradation of Siloxane

Siloxane Photodegradation

A simple static gas reactor was used in order to verify the photocatalytic properties of the synthesized SiO_2/TiO_2 nanomaterial. 0.2 ml HMS was placed into a 115 cm^3 round bottomed flask which was placed in a graphite bath at 130℃. This was to allow the siloxane to fully vaporize, after which 10 ml of the gaseous HMS in air was removed from the round bottomed flask using a syringe and injected into a gas tight ampoule containing a known mass of the photocatalyst. The glass ampoule was then placed in a UV chamber (Figure 2) and GC-FID sampling was used to monitor the concentration of HMS within the ampoule. When the HMS concentration in the ampoule became stabilized, the UV lights (UV_a, with a spectral peak at 365 nm) were turned on. The change in concentration of HMS in the system was monitored until a new equilibrium was reached.

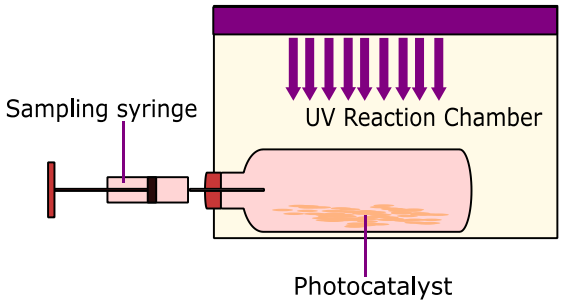

Figure 2: Experimental set up for static gas phase HMS photodecomposition reactions.

Further experiments were performed aimed at studying the lifetime, extended kinetics, and potential SiO_x loading on the TiO_2 catalyst. After observing loss of reactivity in the system, further injection of gaseous HMS in air (10 ml) was made into the airtight vial. A bleed needle was inserted into the ampoule during injection so as to negate increased pressure effects on the photocatalysts as well as to maintain a stable adsorption. After the injection, the concentration of HMS within the system was monitored until it became stable. The UV lights in the photoreaction chamber were then turned on and the HMS concentration was recorded until further stabilisation was reached. HMS/air

injections were repeated until no further HMS decomposition was observed in the presence of UV light.

RESULTS AND DISCUSSION

Characterization data

The created core – shell nanostructures were analysed through scanning electron microscopy (JEOL-JSM 820 scanning microscope), energy dispersive x-ray spectroscopy and x-ray diffraction (Siemens Kristalloflex Diffraktometer using a Cu plate at a wavelength of 1.54Å). The use of SEM imaging allowed to ascertain that the created nanostructure morphology from the electrospinning procedure was indeed of fibrous nature (Figure 3A) and that this structure was not radically changed after the coating procedure (Figures 3B and 3C). It can also be seen in Figure 3C that the specific fibre morphology was very rough after the formation of the TiO_2 coating. In a similar study on the growth of TiO_2 layers on ZnO rods Fan et al. [8] proposed that the origin of the roughness could be attributed to the mismatch between the lattice of the TiO_2 and its substrate which impeded the epitaxial growth of the TiO_2 on the substrate surface. As a consequence of this the TiO_2 shell growth is believed to occur preferentially from a number of nucleation points on the surface rather than grow homogeneously [8-10].

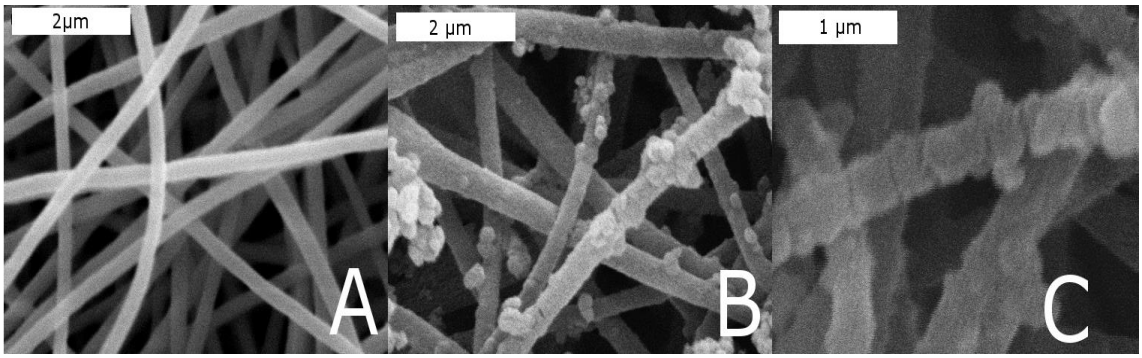

Figure 3: Electron micrographs of pure silica fibres synthesised before (A) and after (B and C) a TiO_2 dip coating procedure involving 10 coating cycles. Figures B and C show the general (B) and specific (C) structures of the newly formed core – shell structures.

It is also important to note the presence of nanocristallites in the core-shell nanostructured mats as can be seen in Figures 3B and 3C. These nanocrystallites are believed to be TiO_2 impurities arising from the dip-coating procedure. Indeed, the natural

high surface area of a nanofibre mat renders it ideal for the trapping of solutions such as water or TTIP mixtures. As a consequence of this high trapping ability it is believed that the cleaning procedure during the formation of the TiO_2 shells is insufficient for the complete removal of excess precursor solution. Upon contact with water the trapped excess solution is then converted into the observed nanocrystallite structures which become less mobile throughout solutions and thus remain stuck within the nanofibre mat. It is believed that the occurrence of these crystals would not impact significantly the photocatalytic activity of the created nanostructures due to their relatively low surface area and adsorption sites. These limited adsorption sites signify that the photodegradation of siloxane species will still occur mainly on the nanofibre surface, thus rendering the overall contribution of the observed nanocrystallites towards siloxane photodegradation, negligible.

From the SEM micrographs of a series of core-shell nanostructured samples, it was possible to establish a growth profile for the thickness of the TiO_2 shell in relation to the number of dip-coating procedures carried out on a given sample. From the growth profile shown in Figure 4 it can be calculated that each individual coating cycle will reliably create a TiO_2 layer with a thickness of 20nm on the coated sample.

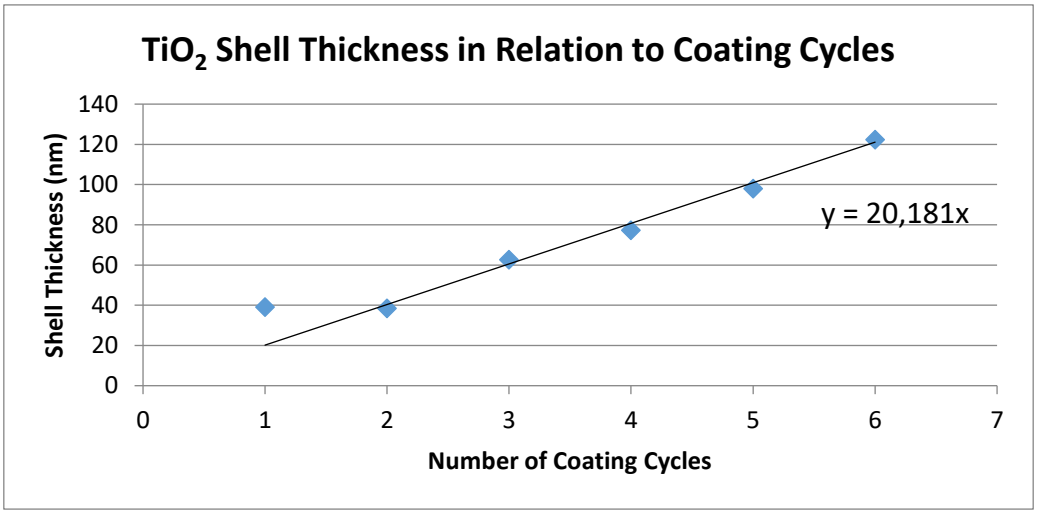

Figure 4: Thickness of TiO_2 shell coating on studied SiO_2/TiO_2 core – shell nanostructures in relation to the number of coating cycles

Figure 5 shows the EDX spectrum of a created core- shell structure created after repeating the dip coating cycle nine times. It is possible to see clearly from Figure 5 that the

analysed sample exhibits both Si and Ti peaks, the Cu peaks observed arise from the substrate on which the fibres were laced during analysis.

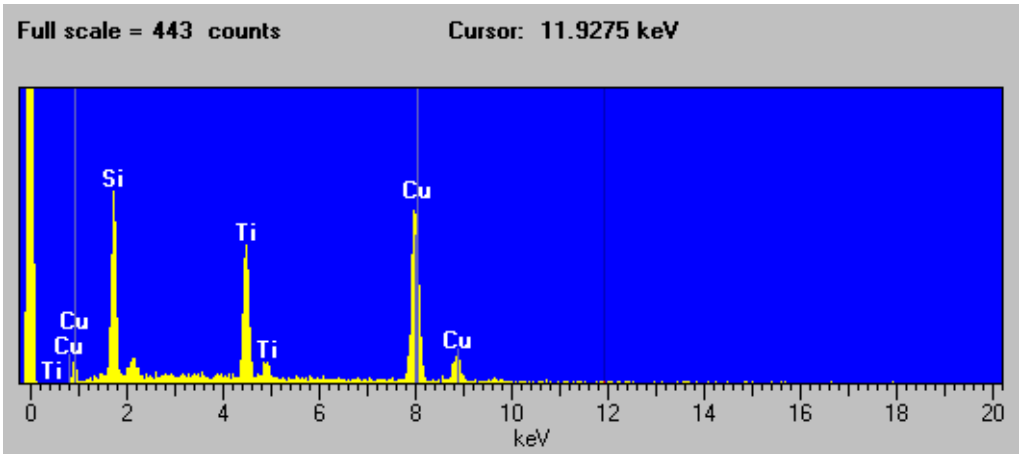

Figure 5: EDX spectrum of SiO_2/TiO_2 core – shell nanofibers after 9 dip coating cycles. The Cu peaks originate from the Cu substrate onto which the fibres were placed for analysis.

Figure 6 shows the XRD spectra of a SiO_2 nanofibre sample before and after the dip coating procedure. From Figure 6, it is possible to note that after the coating procedure, the pattern showing the amorphous structure of the pure SiO_2 nanofibres changes to display the typical pattern of the anatase crystal structure of TiO_2 (identified by correlating the JCPDS database 21-1272). The absence of the rutile phase of TiO_2 is attributed the better stability of the anastase crystal structure which would have been formed preferentially during the thermal conversion of $Ti(OH)_2$ into TiO_2 [9-11]. As such, from Figure 6 it becomes clear that TiO_2 was successfully added to the SiO_2 nanofibre mats through the dip coating procedure.

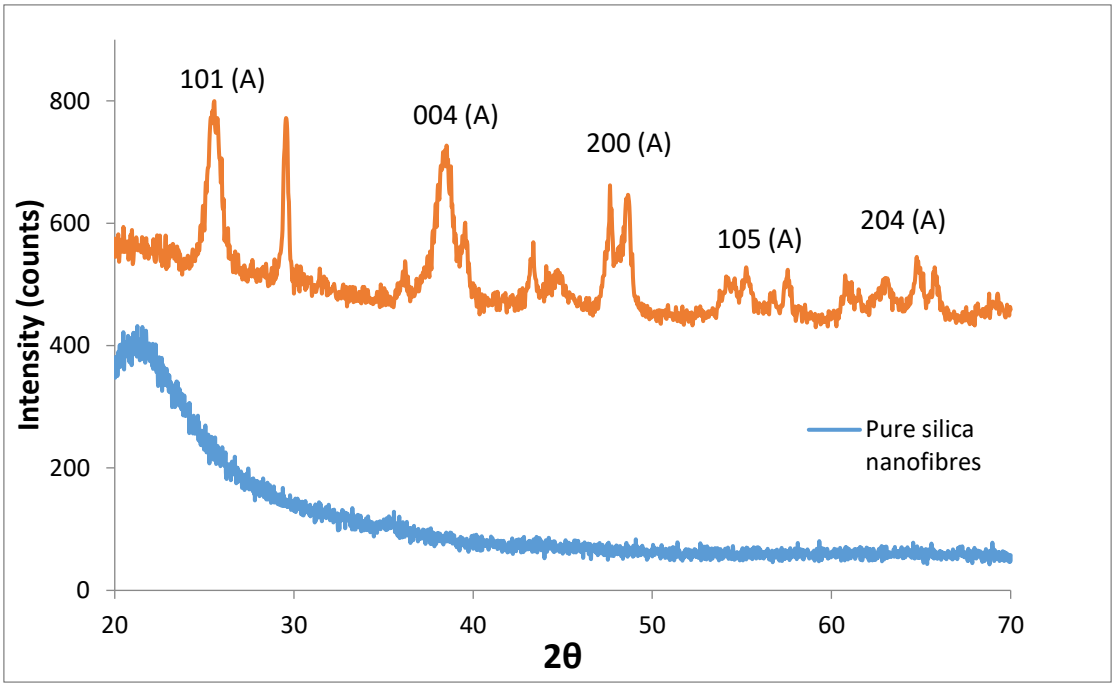

Figure 6: X-ray diffraction patterns showing the amorphous nature of the created SiO_2 nanofibres (below) with respect to the same fibres after the dip-coating procedure. The peak observed at a 2θ value of 21.4 arises from the crystal structure of the calcite substrate onto which the fibres were placed during analysis.

Photodegradation of Siloxanes

As expected, during the evolution of HMS in relation to time and UV illumination in the presence of pure TiO_2 nanofibres, three distinct stages of events were observed. First, the adsorption onto the photocatalysts; second was the photoinduced desorption and lastly, photo-decomposition process. It can be observed from Figure 7, that upon an initial injection of HMS, it rapidly adsorbed onto the surface of the catalyst, which led to its exponential decrease in concentration. Eventually, the adsorption process reached a steady state, leading to a constant HMS concentration, prior to UV irradiation.

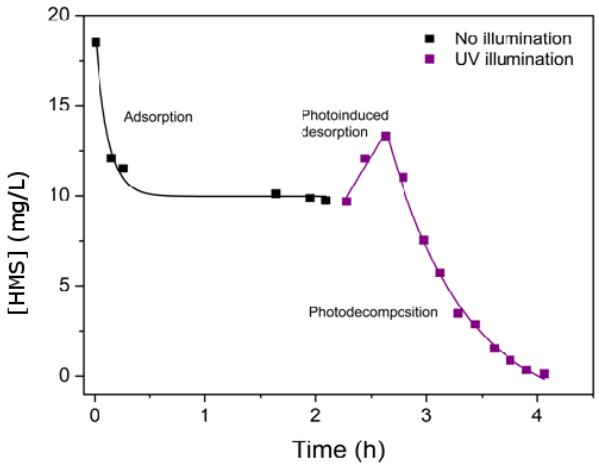

Figure 7: Time and UV illumination dependent evolution of HMS concentration in a static reactor system with pure TiO_2 nanofibres.

A significant increase in HMS concentration can be observed (Figure 7) upon UV illumination, which arises from the photoinduced desorption of HMS from the surface of the photocatalyst. Photoinduced desorption is known to be caused by photonic excitation of the catalyst surface which, becomes more repulsive as a result of the occurring electronic transitions [12]. Photodecomposition occurs concurrently with photoinduced desorption. As also seen in Figure 7, the rate of photodesorption initially remains higher than that of photodegradation, with an increase in HMS concentration within the system. However, as the rate of photodegradation outweighs that of photodesorption, the concentration of HMS drops rapidly. Furthermore, as the time of photodegradation is extended, decline in HMS concentration in the system can be seen which, to follows an exponential decay as shown in Figure 8.

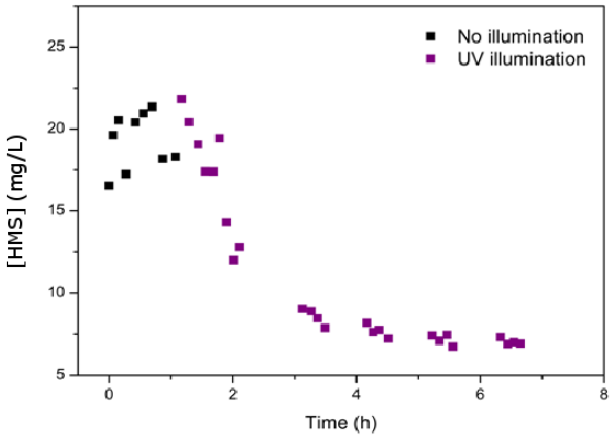

Figure 8: Evolution of HMS concentration in the presence of pure TiO_2 nanofibres in relation to time and UV illumination.

Nevertheless, further extension of the time caused the rate of removal of HMS to plateau due to the consumption of HMS in the system (Figure 8). After undergoing an extensive photo-degradation, the concentration of HMS becomes low enough in such a manner that only a minimal amount of the siloxane will be adsorbed on the TiO_2 surface ultimately causing an overall decrease in photocatalytic activity.

Reaction Mechanism

Ren-De Sun et al [13]. proposed the reaction scheme for the decompositions of siloxanes adsorbed on photoactive TiO_2 shown in equations (1) to (12).

$TiO_2 + h\nu \longrightarrow TiO_2 + e^- + h^+$ **(1)**

$OH^- + h^+ \longrightarrow {}^{\cdot}OH$ **(2)**

$O_{2(ads)} + e^- \longrightarrow O_2^{\cdot}$ **(3)**

$O_2 + H^+ \longrightarrow HO_2{\cdot}$ **(4)**

$\text{-Si-CH}_3 + OH \longrightarrow \text{-Si-CH}_2 + H_2O$ **(5)**

$\text{-Si-CH}_2^{\cdot} + O_2 \longrightarrow \text{-Si-CH}_2OO^{\cdot}$ **(6)**

$\text{-Si-CH}_2OO^{\cdot} + e^- \longrightarrow \text{-Si-CHO} + OH^-$ **(7)**

$\text{-Si-CHO} + {}^{\cdot}OH \longrightarrow \text{-Si-CO}^{\cdot} + H_2O$ **(8)**

$$\text{-Si-CO}^{\cdot} + O_2 \longrightarrow \text{-Si-(CO)OO}^{\cdot} \quad \textbf{(9)}$$

$$\text{-Si-(CO)OO}^{\cdot} + H_2O \longrightarrow \text{-Si-(CO)OOOOH} \longrightarrow \text{-Si-(CO)O}^{\cdot} + O_2 + {}^{\cdot}OH \quad \textbf{(10)}$$

$$\text{-Si-(CO)O}^{\cdot} \longrightarrow \text{-Si}^{\cdot} + CO_2 \quad \textbf{(11)}$$

$$\text{-Si}^{\cdot} + {}^{\cdot}OH \longrightarrow \text{-SiOH} \quad \textbf{(12)}$$

Although TiO_2 photocatalysis was established as a theoretically viable mean for the removal of siloxanes from biogas, the created SiO_x species on the TiO_2 surface was seen to be detrimental to the longevity of the catalyst. Indeed, studies by Hay et al. [14] demonstrated that as the photodecomposition process was carried out for extended periods of time (up to 18 months of continual use) SiO_x deposits were seen to form on the photocatalysts. At low concentrations, these deposits only lowered the photocatalytic efficiencies of the created filter systems but at higher concentrations, the deposited SiO_x layer was seen to effectively act as an insulator, preventing electron mobility from the catalyst to surface adsorbed species, and thus effectively neutralising the catalyst [15-19].

Nonetheless, the main limitations for the use of TiO_2 as a photocatalyst for the removal of siloxanes from biogas are not due to the poisoning of the catalyst, an issue which can easily be overcome through the use of a variety of techniques [20-23], but due to the relatively low efficiency of this method for the removal of siloxanes in biogas. Indeed, although the use of a photocatalyst for the decomposition of siloxanes would allow for a more facile removal technique compared to those already in use, such a system cannot yet withstand the intensive use required by industrial processes. These limitations, however, could be resolved by the use of nanostructured TiO_2 materials which offer a considerable series of advantages compared to their macroscale counterparts.

CONCLUSION

In conclusion, it is possible to say that the initial studies presented in this study towards the construction of metal oxide nanocatalysts for photodegradation of siloxanes in biogas were successful. However, the specific control of the material morphology and its effects on the photocatalytic efficiency for the degradation of siloxanes in biogas are subjects that remain to be investigated. As such the synthesis of TiO_2 nanostructures was deemed as an

essential progression for modern siloxane photodegradation technologies and their applicability in industrial situations. Electrospun nanofibres have inherent high surface area and facile synthesis procedures. Through the use of SEM, EDX and XRD analytical techniques it was possible to successfully characterise the created nanostructures and determine that the developed procedure allowed the synthesis of SiO_2/TiO_2 core – shell nanofibres within a narrow diameter range. SiO_2/TiO_2 core – shell nanofibres eliminated the fragility of titania nanofibres, which has been a major drawback and significantly limits the applicability of pure TiO_2 nanofibres for industrial applications. Furthermore, the facile experimental technique used for the synthesis of these structures was demonstrated to allow for a fine control over the thickness of the TiO_2 shell on the silica nanofibres.

The ability to successfully create a controlled TiO_2 shell on SiO_2 is one of essential interest in the photodegradation of siloxanes. Indeed, one of the major issues displayed by TiO_2 photocatalysts during the degradation of siloxane species is the poisoning of the catalyst. This poisoning is known to occur as a consequence of the accumulation of silica microscristallites on the surface which are created as a consequence of siloxane photodegradation. Thus, by using the coating technique presented in this work it would be simple to create a novel photoactive layer on poisoned catalyst surfaces, thus creating a facile photocatalyst regeneration technique which could be highly appealing from an industrial perspective.

REFERENCES

[1] E. A. Gorrepati, P. Wongthahan, S. Raha and H. S. Fogler (2010), Silica precipitations in acidic solutionsmechnism, pH effects and salt effect. *Langmuir*, **26**, 10467–74.

[2] J. L. Gurav, A. V. Rao, A. P. Rao, D. Nadargi and S. Bhagat (2009), Physical properties of sodium silicate based silica aerogels prepared by single step sol-gel process dried at ambient pressure *J. Alloys Compd.*,**476**, 397–402.

[3] S. H. Garofalini and G. Martin, (1994), Sol-gel polymerization: analysis of molecular mechanisms and the effect of hydrogen *J. Phys. Chem.*, 98, 1311–1316**.**

[4] G. R. Choppin, P. Pathak and P. Thakur, (2008), polymerization and complexation behaviuor of silicic acid. *Main Gr. Met. Chem.*, **31**, 53–71.

[5] R. Deshpande, D.-W. Hua, D. M. Smith and C. J. Brinker,(1992), Pore structure evolution in silica gel during aging/drying*J. Non. Cryst. Solids*, **144**, 32–44.

[6] P. J. Davis, C. Jeffrey Brinker, D. M. Smith and R. A. Assink, (1994), Pore structure evolution in silica gel during aging/drying. IV. Varying pore fluid pH *J. Non. Cryst. Solids*, **142**, 197–207.

[7] R.K Bordia and G. W. Scherer,(1988), On constrained sintering—I. Constitutive model for a sintering body *Acta Metallurgica*, 36, (9) 2393–2397**.**

[8] J. Fan, R. Zamani, C. Fábrega, A. Shavel, C. Flox, M. Ibáñez, T. Andreu, A. M López, J. Arbiol, J. R. Morante (2012) Solution-growth and optoelectronic performance of ZnO : Cl/TiO_2 and ZnO : Cl/Zn*x*TiO*y*/TiO_2 core–shell nanowires with tunable shell thickness 2012 *J. Phys. D: Appl. Phys.* 45 415301

[9] S. D. Bhagat, Y.-H. Kim, Y.-S. Ahn and J.-G. Yeo,(2006), Textural properties of ambient pressure dried water-glass based silica aerogel beads: One day synthesis ***Microporous*** *Mesoporous Mater,* 96, (1-3) 237–244.

[10] J. V. Alemán, A. V. Chadwick, J. He, M. Hess, *et al*, ,(2007), Definitions of terms relating to the structure and processing of sols, gels, networks, and inorganic-organic hybrid materials (IUPAC Recommendations 2007) *Pure Appl. Chem.*, 79, 1801–1829.

[11] D. R. Ortega and A. Subrenat,(2009), Siloxane treatment by adsorption into porous materials *Environ. Technol.*, **30**, 1073–1083.

[12] M. C. Canela, R. M. Alberici and W. F. Jardim,(1998), Gas-phase destruction of H_2S using TiO_2/UV-Vis *J. Photochem. Photobiol. A Chem.*, **112**, 73–80.

[13] S. H. Lim, N. Phonthammachai, S. S. Pramana, and T. J. White (2008) Simple Route to Monodispersed Silica−Titania Core−Shell Photocatalysts *Langmuir 24* (12), 6226-6231

[14] S.O Hay, T.N Obee, C. Thibaud-Erkey (2010) The deactivation of photocatalytic based air purifiers by ambient siloxanes United States Environmental Protection Agency 99 (3-4); pp 435-441

[15] K. Karthik, S. K. Pandian and N. V. Jaya,(2010), Effect of nickel doping on structural, optical and electrical properties of TiO_2 nanoparticles by sol–gel method *Appl. Surf. Sci.*, 256, 6829–6833.

[16] M. Bellardita, M. Addamo, A. Di Paola and L. Palmisano,(2007), Photocatalytic behaviour of metal-loaded TiO_2 aqueous dispersions and films *Chem. Phys.*, 339, 94–103.

[17] X. Li, F. Wang, Q. Qian, X. Liu, L. Xiao and Q. Chen,(2012), Ag/TiO2 nanofibers heterostructure with enhanced photocatalytic activity for parathion Mater. Lett., 66, 370–373.

[18] A. Ivask, T. Titma, M. Visnapuu, H. Vija, et al.,(2015), Toxicity of 11 Metal Oxide Nanoparticles to Three Mammalian Cell Types In Vitro Curr. Top. Med. Chem., 15, 1914–29.

[19] J. H. Park, O. O. Park and S. Kim,(2006), Photoelectrochemical water splitting at titanium dioxide nanotubes coated with tungsten trioxide Appl. Phys. Lett., 89, 163106.

[20] T. Putta, M.-C. Lu and J. Anotai,(2011), Photocatalytic activity of tungsten-doped TiO2 with hydrothermal treatment under blue light irradiation J. Environ. Manage., 92, 2272–2276.

[21] O. Lorret, D. Francová, G. Waldner and N. Stelzer,(2009) W-doped titania nanoparticles for UV and visible-light photocatalytic reactions Appl. Catal. B Environ., 91, 39–46.

[22] H. Song, H. Jiang, X. Liu and G. Meng,(2006), Efficient degradation of organic pollutant with WOx modified nano TiO2 under visible irradiation J. Photochem. Photobiol. A Chem., 181, 421–428.

[23] H. Aizawa and S. Tsuneyuki,(1996), First-principles investigation of photo-induced desorption of CO and NO from Pt(111) Surf. Sci., 363, 223–228.